Nature Environment and Pollution Technology
An International Quarterly Scientific Journal

p-ISSN: 0972-6268
e-ISSN: 2395-3454

Vol. 16 | No. 2 | pp. 479-484 | 2017

Original Research Paper | Open Access

Co-metabolism Degradation of Pyridine with Glucose in Sequencing Batch Biofilm Reactor (SBBR)

Jingzhou Quan, Yancheng Li, Qinglin Sun and Jian Zhou†
Key Laboratory of the Three Gorges Reservoir's Eco-Environments, Chongqing University, Chongqing, 400045, P.R. China
†Corresponding author: Jian Zhou

Nat. Env. & Poll. Tech.
Website: www.neptjournal.com

Received: 12-05-2016
Accepted: 16-07-2016

Key Words:
Pyridine
Co-metabolism
Dissolved oxygen (DO)
PCR-DGGE

ABSTRACT

Biological treatment of pyridine wastewater is difficult because of it's poor biodegradability. In order to deal with the problem, this study applied glucose as co-metabolism growth substrate to build co-metabolism system for biological degradation of pyridine in Sequencing Batch Biofilm Reactor (SBBR). The study investigated the effect of dissolved oxygen (DO) on the system building. The result showed that DO had significant influence on the establishment of the system. When the pyridine loading was 0.5 kg COD m^{-3} d^{-1} and the glucose loading rate was 1.0 kg COD m^{-3} d^{-1}, the most suitable DO was 3.5 mg/L. After 70 days operation, the pyridine removal efficiency reached stable, which was 83.6%. Meanwhile, under the condition that DO was 3.5 mg/L, pyridine loading had an effect on pyridine removal efficiency. The favourable pyridine loading was 0.5 kg COD m^{-3} d^{-1}. PCR-DGGE illustrated that the microbial community varied under different DO concentrations. Compared with seed sludge, the similarity were 50.2%, 44.1%, 35.8% and 62.9% respectively, when DO were 0.5, 2.0, 3.5 and 5.0 mg/L. Fourier transforms infrared spectroscopy (FTIR) results showed that primary amides and carboxylic acids generated in effluent as intermediate products during pyridine degradation process.

INTRODUCTION

Pyridine is a kind of refractory organic substance belonging to nitrogen-containing heterocyclic compounds, which is commonly existing in coking wastewater, refinery wastewater and pesticide wastewater (Varela & Saá 2003). It is a sensitive pollutant in the environment, because it can cause deformity and is toxic to human and aquatic species (Qiao & Wang 2010). Currently, common technologies developed for pyridine degradation focus on two main ways: physico-chemical treatment technology and biological treatment technology. Physico-chemical treatment technologies for pyridine degradation include incineration, adsorption, absorption power and advanced oxidation (Ghose 2002), which works well. However, high investment and operating costs, complicated operation and management and secondary pollution of by-products make it a less attractive method. Biological treatment technology is cost-effective and environment-friendly, but the removal efficiency remains low for pyridine degradation by using traditional biological methods. Recently, many new methods have been emerged such as biofortification or biological additive technology (*Paracoccus* sp. KT-5 (Lin et al. 2010), *Pseudomonas pseudoalcaligenens*-KPN (Padoley et al. 2006) and *Nocardiodes* sp. BS001 (Bai et al. 2008), which can enhance removal efficiency significantly. However, continuous dosing is needed, because of short acting time. Recently, much attention has been paid to co-metabolism technology for refractory organic degradation. Kweon et al. (2011) found that pyrene has been observed to complete biodegradation to CO_2 (biomineralisation) in the fast-growing *Mycobacterium vanbaalenii*. Zhong et al. (2010) revealed that *Cycloclasticus* sp. can use phenanthrene as growth substrates to co-metabolic bio-degradate pyrene. Zhou et al. (2011) investigated that *Pseudomonas oleovorans* can use tetrahydrofuran as growth substrates to co-metabolic bio-degradate oleovorans.

The aim of the study was to build a biological co-metabolism system to degrade pyridine by choosing glucose as the growth substrate and investigate the effect of dissolved oxygen (DO) on its establishment. PCR-DGGE was used to compare the difference of microbial community under different DO concentration. When the system was stable, the study investigated the effect of pyridine loading on the removal efficiency. Fourier transforms infrared spectroscopy (FTIR) was used to detect the change of pyridine after treatment.

MATERIALS AND METHODS

Bioreactor: The SBBR (Fig. 1) was designed for 12 L of working volumes, with a dimension of 30 cm height and 25

cm diameter. The reactor was filled with combination packing fillings (constituted by hanging 6 g ~ 7 g white semi-flexible filiform materials on each disc). The fill ratio was 40%. Temperature was adjusted by incubator, oxygen was pumped into each reactor by air pump. The operational mode is "influent 0.5 h-reaction 22.5 h-sedimentation 0.5 h - effluent 0.5 h".

Chemicals: Pyridine wastewater was replaced and imitated by artificial water, experimental reagents were analytical grade or pure class distinctions, among which pyridine (AR grade) was produced by Aladdin. The microelements were added as nutrient supplement in the experiment. The microelement doses were as mentioned in Table 1.

Experimental procedure: The influence of DO on system building was investigated through conducting parallel tests. SBBRs were seeded by the sludge (10 g/L TSS). The temperature was kept as a constant (30 °C ± 0.5 °C), the pyridine loading rate was 0.5 kg COD m^{-3} d^{-1} and the glucose loading rate was 1.0 kg COD m^{-3} d^{-1}. Under the same experimental conditions, DO was adjusted to 0.5, 2.0, 3.5 and 5.0 mg/L in different SBBRs, respectively. And PCR-DGGE was used to analyse the microbial communities. Under the condition that DO was 3.5 mg/L, the removal efficiency for different pyridine loading was investigated.

Wastewater quality analysis: COD was analysed with potassium dichromate digestion method (HACH DRB200 and HACH DR2800), TOC was analysed with UV-light catalytic oxidation (ElementarLiqui TOC, Germany), and temperature and ORP were monitored by a portable multi parameter digital analyser (HQ40d).

Pyridine concentration was measured by ultraviolet (UV)-visible spectrophotometer (DR5000; Hach, USA) with an absorption wavelength of 276 nm. Linear relation between pyridine concentration (C) and absorbance value (A) was C = 28.226 A, R^2 = 0.9994 (C: 0 mg/L to 160 mg/L).

The effluent was collected for Fourier transform infrared spectroscopy (FTIR) study. Process: Take 100 mL sample, frozen it to a solid state and powdered by vacuum freeze drier; mix the powder (1~2 mg) and KBr (300 mg), ground it with pestle and mortar (less than 2 microns) in infrared light, and pressed into slice under (5~10)×10^7 Pa for about 1 min. The spectra were collected using FTIR system equipped with diffuse reflectance accessory in a range of 400-4000 cm^{-1}.

Polymerase chain reaction-denaturing gradient gel electrophoresis analysis: Biofilms were taken from the SBBRs. Biological sample was placed into a 2.0 mL Eppendorf tube in accordance with the quantity of samples. The method of PCR-DGGE was the same as that used by Zhang et al. (2014), and then, the extracted DNA samples was amplified by PCR. Primers were V3:F-357-GC (GC-clamp-CCCATACGG GAGGCAGCAG), V3:R-518 (ATTACCGCGGCTGCTGG). Products were analysed by American Bio-Rad's Gene Mutation Detection System (The DcodeTM Universal Mutation Detection System) and the image was analysed by BIO-RAD QUANTITY ONE.

RESULTS AND DISCUSSION

Influence of DO on pyridine biological system building: As is shown in Fig. 2 and Fig. 3, pyridine removal efficiency was poor and the variation curve was flat in the first 20 days. After a period of adaptation, removal efficiency had been significantly enhanced in 30~80 days. The removal efficiency reaches stable on day 60, 70 and 80, when DO were

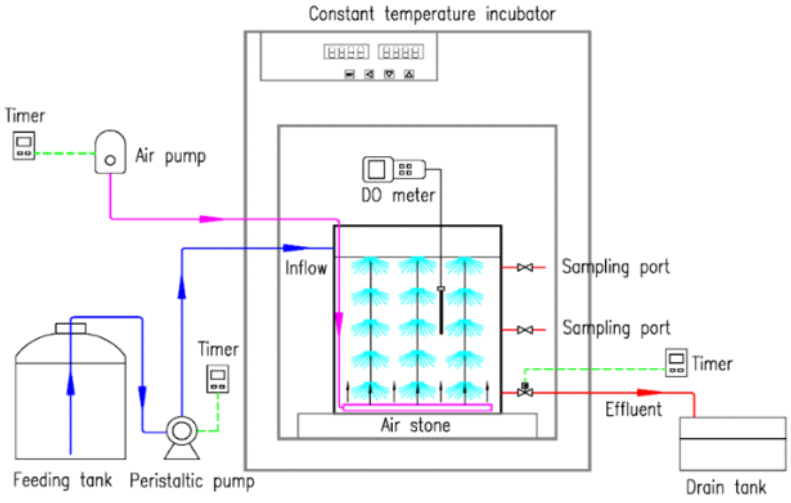

Fig. 1: Schematic diagram of SBBR.

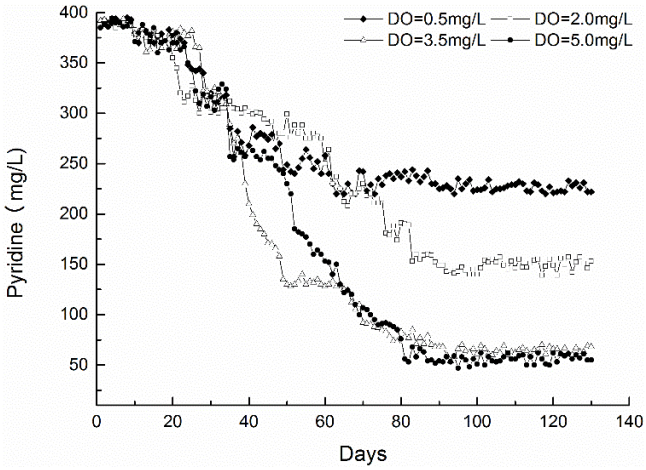

Fig. 2: Diurnal variation curve of DO on pyridine.

Table 1: The microelement doses of reactor.

No.	Microelement	Concentration/(mg/L)
1	$MgSO_4 \cdot 7H_2O$	12.32
2	$CaCl_2$	0.56
3	$COCl_2 \cdot 6H_2O$	0.41
4	$Na_2MoO_4 \cdot 2H_2O$	1.26
5	$FeSO_4 \cdot 7H_2O$	2.50
6	$ZnSO_4 \cdot 7H_2O$	0.43
7	$MnSO_4$	0.76

Table 2: The result of infrared spectroscopic analysis.

No.	wavelength/cm^{-1}	Group vibration Description
1	660	H_2O swing
2	901	NH_2 distortion
3	1190	Carboxylic acid C-OH stretching
4	1415	C-N stretching of R-$CONH_2$ primary amides
5	1730	Hydroxy carboxylic acid C = O stretching
6	3180	Aromatics = C-H stretching
7	3400	Carboxylic acid dimer OH stretching

0.5, 3.5 and 5.0 mg/L respectively. The results illustrated that the influence of DO on pyridine biological system building (Parikh et al. 2011) is significant. When pyridine biological system performed stable (Fig. 3), the corresponding ORP of the system were 42.9, 107.5, 116.7 and 130.0 mV respectively. As DO concentration increased, pyridine and TOC degradation rate showed a trend of increase, especially when DO was more than 3.5 mg/L. However, the removal efficiency of both pyridine and TOC did not increase so dramatically as the DO concentration exceeded 3.5 mg/L. Pyridine and TOC degradation rate was only increased by 2.93% and 0.20%. So the suitable DO was 3.5 mg/L in this pyridine degradation system. The possible cause would be that suitable microbial growth environment was built under suitable DO level, achieving an efficient degradation of pyridine.

The system efficiency of pyridine loading in pyridine co-metabolism system: The experiment kept DO a constant (3.5 mg/L), adding glucose (1.0 kg COD m^{-3} d^{-1}) as co-metabolism substrates (Fig. 4). When pyridine loadings were 0.2, 0.5, 1.0 and 2.0 kg COD m^{-3} d^{-1}, corresponding pyridine degradation rates were 84.1%, 83.6%, 53.2% and 38.3% respectively, and TOC were 85.9%, 82.2%, 66.9% and 53.0% respectively. As the pyridine loading increased, the pyridine and TOC removal efficiency decreased, all of which might be caused by the inhibition of microbial growth under high pyridine loading (Bai et al. 2009). The most efficient pyridine loading was 0.5 kg COD m^{-3} d^{-1}, since the pyridine and TOC removal efficiency did not enhance so obviously, when the pyridine loading was less than 0.5 kg COD m^{-3} d^{-1}.

Infrared spectrum analysis of pyridine degradation: The effluent was analysed by FTIR while DO and pyridine loading were 3.5 mg/L and 0.5 kg COD m^{-3} d^{-1}. The results (Fig. 5 and Table 2) showed that, wavelength of 1415, 3400, 1190, 1730 and 901 cm^{-1} were new wave peaks, which represented primary amides and carboxylic acid functional groups respectively. The primary amides and carboxylic acids in effluent were generated from pyridine degradation process in the co-metabolism system. Mono oxygenase reaction was one of the reactions for pyridine degradation, during which -OH can be added on pyridine ring (Dahlen & Rittmann 2002). Besides, pyridine ring also can be broken down and organic nitrogen of pyridine was converted to NH_4^+ during pyridine degradation (Feng et al. 2013). These processes can produce intermediates such as primary amides and carboxylic acid. Qiao et al. (2011) and Bocarsly et al. (2012) stated that generated carboxylic acid was glutaric acid and formic acid during pyridine biodegradation. Carboxylic acid C-OH stretching might be caused by glucose and aromatics = C-H stretching might be caused by pyridine functional groups.

Analysis of pyridine degraded microbial groups: The results of microbial groups are shown in Fig. 6. Land 1 was seed sludge. Land 2, Land 3, Land 4 and Land 5 were sludge samples with DO from 0.5 to 5.0 mg/L. Compared with Land 1, the similarity of microbial groups were 50.2%, 44.1%, 35.8% and 62.9% respectively. The largest similarity occurred when DO was 5.0 mg/L, while the smallest one occurred when DO was 3.5 mg/L. The amount of bands under different DO concentration were 23, 23, 25 and 28 respectively. The species richness of microbial groups increased as DO level went up. So DO level had a significant effect on microbial community. Since ORP was different under different DO levels, which created a different environment (Lu

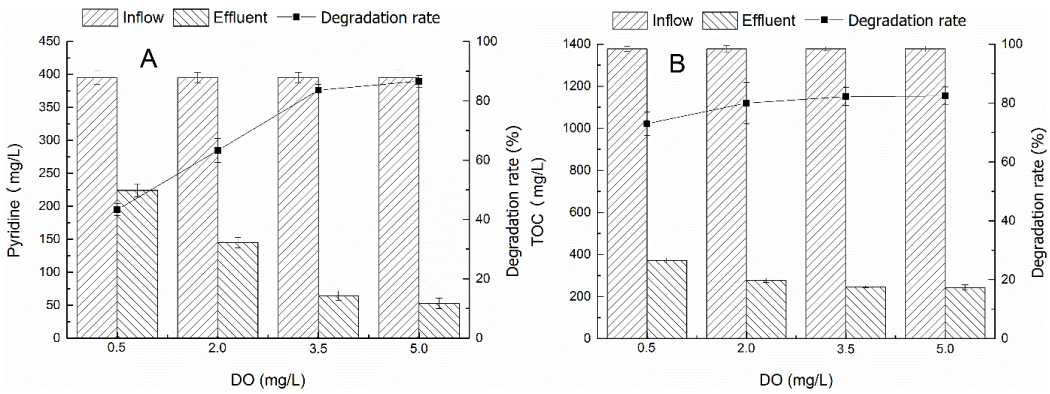

Fig. 3: Effect of DO on pyridine(A) and TOC(B) removal.

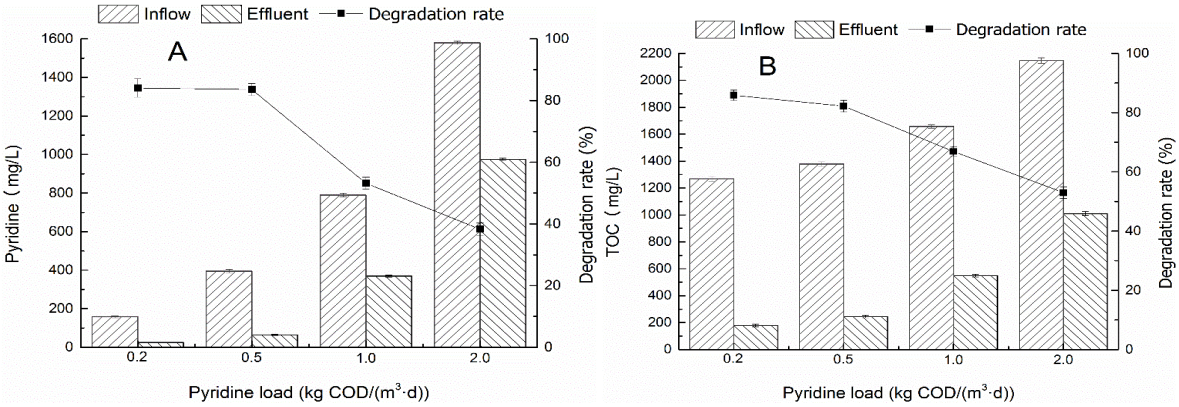

Fig. 4: Effect of pyridine load on pyridine(A) and TOC(B) removal.

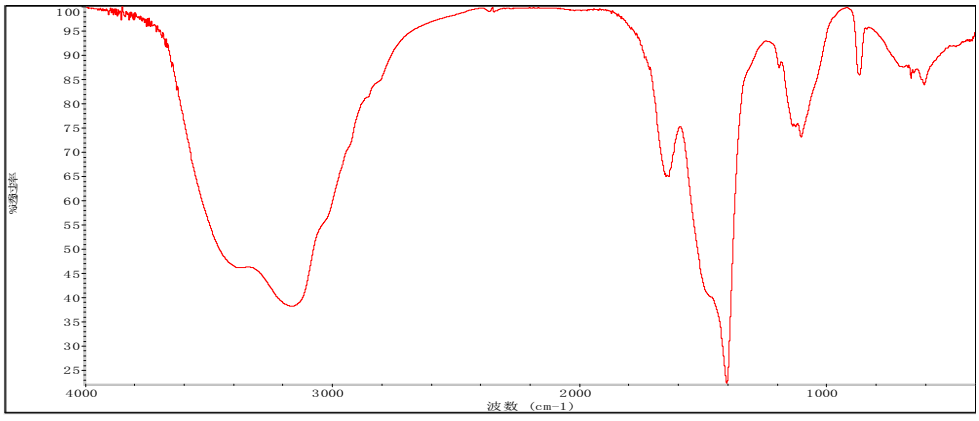

Fig. 5: The infrared spectrum of pyridine.

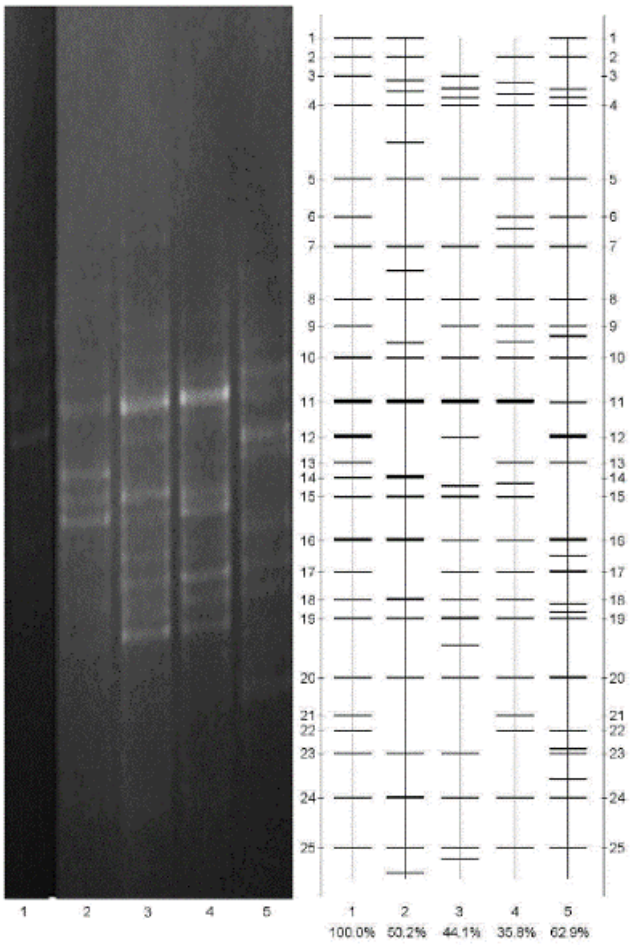

Fig. 6: DGGE profiles of biofilm samples (Land 1: seed sludge (Land 2: DO=0.5 mg/L, Land 3: DO=2.0 mg/L, Land 4: DO=3.5 mg/L, Land 5: DO=5.0 mg/L).

et al. 2010) for certain microbial species growth. As a result, pyridine removal efficiency varied under different DO levels.

CONCLUSIONS

With glucose as growth substrate, co-metabolism system for pyridine degradation could be built successfully. The pyridine removal efficiency increased at first and then kept stable. The co-metabolism system can effectively remove pyridine. DO affected the building process. As DO level gradually increased, pyridine removal efficiency increased. Under suitable DO level, higher pyridine loading would inhibit the microbial growth in co-metabolism system resulting in low removal efficiency. The most efficient pyridine loading was 0.5 kg COD m^{-3} d^{-1}. According to results of FTIR, new functional groups emerged in effluent after pyridine degradation process. The main generated products were carboxylic acids and primary amides substance. The PCR-DGGE results indicated that the microbial community developed from the same seed sludge was different under different DO levels. The research topic has valuable implications on the bioremediation of pyridine.

ACKNOWLEDGEMENT

This work was supported by the National Water Pollution Control and Management of Science and Technology major projects under Grant No. 2009ZX07315-005.

REFERENCES

Bai, Y., Sun, Q., Zhao, C., Wen, D. and Tang, X. 2008. Microbial degradation and metabolic pathway of pyridine by a *Paracoccus* sp. strain BW001. Biodegradation, 19(6): 915-926.

Bai, Y., Sun, Q., Zhao, C., Wen, D. and Tang, X. 2009. Simultaneous biodegradation of pyridine and quinoline by two mixed bacterial strains. Applied Microbiology and Biotechnology, 82(5): 963-973.

Bocarsly, A.B., Gibson, Q.D., Morris, A.J., L'Esperance, R.P., Detweiler, Z.M., Lakkaraju, P.S., Zeitler, E.L. and Shaw, T.W. 2012. Comparative study of imidazole and pyridine catalyzed reduction of carbon dioxide at illuminated iron pyrite electrodes. ACS Catalysis, 2(8): 1684-1692.

Dahlen, E.P. and Rittmann, B.E. 2002. Two-tank suspended growth process for accelerating the detoxification kinetics of hydrocarbons requiring initial monooxygenation reactions. Biodegradation, 13(2): 101-116.

Feng, G., Lian, Y.Y., Yang, D., Liu, J. and Kong, D. 2013. Distribution of Al and adsorption of NH_3 and pyridine in ZSM-12: A computational study. Canadian Journal of Chemistry, 91(10): 925-934.

Ghose, M. 2002. Complete physico-chemical treatment for coke plant effluents. Water Research, 36(5): 1127-1134.

Kweon, O., Kim, S.J., Holland, R.D., Chen, H., Kim, D.W., Gao, Y., Yu, L.R., Baek, S., Baek, D.H. and Ahn, H. 2011. Polycyclic aromatic hydrocarbon-metabolic network in Mycobacterium vanbaalenii PYR-1. Journal of Bacteriology, JB-00215.

Lin, Q., Donghui, W. and Jianlong, W. 2010. Biodegradation of pyridine by Paracoccus sp. KT-5 immobilized on bamboo-based activated carbon. Bioresource Technology, 101(14): 5229-5234.

Lu, Z.H., Zhang, Y., Li, L.T., Curtis, R.B., Kong, X.L., Fulcher, R.G., Zhang, G. and Cao, W. 2010. Inhibition of microbial growth and enrichment of α-aminobutyric acid during germination of brown rice by electrolyzed oxidizing water. Journal of Food Protection, 73(3): 483-487.

Padoley, K., Rajvaidya, A., Subbarao, T. and Pandey, R. 2006. Biodegradation of pyridine in a completely mixed activated sludge process. Bioresource technology, 97(10): 1225-1236.

Parikh, C., Trivedi, H. and Livingston, D. 2011. A decade of simultaneous nitrification and denitrification experience in over 60 conventional and MBR applications-lessons learned. Proceedings of the Water Environment Federation, 2011(13): 3629-3655.

Qiao, L. and Wang, J.l. 2010. Microbial degradation of pyridine by *Paracoccus* sp. isolated from contaminated soil. Journal of Hazardous Materials, 176(1): 220-225.

Qiao, N., Li, M., Schlindwein, W., Malek, N., Davies, A., Trappitt, G. 2011. Pharmaceutical cocrystals: an overview. International Journal of Pharmaceutics, 419(1): 1-11.

Varela, J.A. and Saá, C. 2003. Construction of pyridine rings by metal-mediated [2+ 2+ 2] cycloaddition. Chemical Reviews, 103(9): 3787-3802.

Zhang, J., Zhou, J., Han, Y. and Zhang, X. 2014. Start-up and bacterial communities of single-stage nitrogen removal using anammox and partial nitritation (SNAP) for treatment of high strength ammonia wastewater. Bioresource Technology, 169: 652-657.

Zhong, Y., Zou, S., Lin, L., Luan, T., Qiu, R. and Tam, N.F. 2010. Effects of pyrene and fluoranthene on the degradation characteristics of phenanthrene in the cometabolism process by Sphingomonas sp. strain PheB4 isolated from mangrove sediments. Marine Pollution Bulletin, 60(11): 2043-2049.

Zhou, Y.Y., Chen, D.Z., Zhu, R.Y. and Chen, J.M. 2011. Substrate interactions during the biodegradation of BTEX and THF mixtures by *Pseudomonas oleovorans* DT4. Bioresource Technology, 102(12): 6644-6649.